Mechanistic Aspects of Stannole Formation Catalyzed by the Phosphine-Coordinated Transition-Metal Complexes $M(PR_3)_2$: An ab Initio MO Study

Riadh Sahnoun, Toshiaki Matsubara,* and Tokio Yamabe

Institute for Fundamental Chemistry, 34-4 Takano-Nishihiraki-cho, Sakyo-ku, Kyoto 606-8103, Japan

Received June 12, 2000

The reaction mechanism of the [2 + 2 + 1] cycloaddition of two ethynes and one stannylene, SnR'_2 (R′ = H, $CH(SiMe_3)_2$), to produce stannole catalyzed by the transition-metal complexes $M(PR_3)_2$ (**1**; M = Ni, Pd, Pt; R = H, Me, i-Pr, t-Bu) has been theoretically investigated by means of both density functional theory (DFT) and ONIOM methods. The DFT calculations of the model molecule with R and R′ = H showed that the catalytic reaction proceeds via the 1,2-metallastannete intermediate **4**, as experimentally proposed. The starting complex **1** first reacts with stannylene to from the stannylene complex **5**, which is followed by ethyne addition to the M−Sn double bond with a small energy barrier of less than 10 kcal/mol for all three metals to form **4**. The subsequent ethyne insertion into the M−Sn bond and the C−C bond formation, which require the larger energy barrier, take place to produce stannole. For Ni and Pd, the ethyne insertion needs the largest energy barrier of 11.3 and 16.4 kcal/mol, respectively. On the other hand, the C−C bond formation needs the largest energy barrier of 21.9 kcal/mol for Pt. For all three metals, the transition state **TS2** in the ethyne addition to the M−Sn double bond was located at the highest point on the entire potential energy surface. On the basis of the potential energy surface, the sequence of catalytic activity Ni > Pd > Pt was found. We also examined with the ONIOM method the electronic and steric effects of the substituents of the phosphine ligand on the potential energy surface of the ethyne insertion and the C−C bond formation which have the large energy barrier using the real molecule with R′ = $CH(SiMe_3)_2$ and R = Me, i-Pr, t-Bu for Pd. It was predicted that with an increase in the bulkiness of R the energy barrier in the ethyne insertion is reduced and becomes smaller than that in the C−C bond formation, switching the step which has the highest energy barrier. The highest catalytic activity of the substituent i-Pr was also suggested.

1. Introduction

The chemistry of transition-metal−tin complexes has been an active area of experimental research for a long time, because of their catalysis applicable to various important synthetic reactions, such as hydrogenation, reduction under water-gas shift conditions, hydroformylation, coupling, and so on.[1] The unique properties of the metal−tin bond also have attracted much attention from experimental chemists and have been investigated by the various experimental techniques.[1] The synthesis of metalloles by transition-metal complexes was one challenging subject over the last four decades, because the metalloles, which belong to the general class of heteroles (i.e., heterocyclopenta-2,4-dienes) can be applied to both biological and chemical processes and also to the production of new electrical conductors.[2] Nevertheless, only a few compounds have been synthesized under vigorous conditions without catalyst so far. In contrast, with transition-metal catalysts, a noticeable improvement has been made in the synthesis of a variety of metalloles of groups 14−16.

Recently, a [2 + 2 + 1] cycloaddition reaction of two ethynes and one stannylene, SnR'_2 (R′ = $CH(SiMe_3)_2$ and R'_2 = $\{C(SiMe_3)_2CH_2\}_2$), catalyzed by the phosphine-coordinated palladium complexes $Pd(PR_3)_2$ and $Pd(R_2PC_2H_4PR_2)$ (R = Me, i-Pr, t-Bu) to form the stannoles $(C_4H_4)SnR'_2$ at a low temperature was reported by Pörschke and co-workers.[3] A mechanism of the entire catalytic cycle can be proposed as depicted in Figure 1 on the basis of their experimental results.

In the first process of the entire catalytic cycle, the formation of the 1,2-metallastannete intermediate **4**, we consider the two reactions denoted by paths a and b, because the reactant **1** can give the two adducts **2** and **5** by reactions with ethyne and SnR_2, respectively. In path a, the reactant **1** first reacts with ethyne to form the ethyne complex **2**, followed by the reaction with SnR'_2 leading to **4**. On the other hand, in path b, the stannylene complex **5** is first formed by the reaction of **1** with SnR'_2 and then **4** is formed by the reaction with C_2H_2. In the subsequent reaction starting from **4**, also the alternative paths c and d can be considered,

(1) Holt, M. S.; Wilson, W. L.; Nelson, J. H. *Chem. Rev.* **1989**, *89*, 11 and references therein.
(2) Dubac, J.; Laporterie, A.; Manuel, G. *Chem. Rev.* **1990**, *90*, 215.
(3) (a) Krause, J.; Pluta, C.; Pörschke, K.-R.; Goddard, R. *J. Chem. Soc., Chem. Commun.* **1993**, 1254. (b) Krause, J.; Haack, K.-J.; Pörschke, K.-R.; Gabor, B.; Goddard, R.; Pluta, C.; Seevogel, K. *J. Am. Chem. Soc.* **1996**, *118*, 804.

10.1021/om000487k CCC: $19.00
Publication on Web 11/18/2000

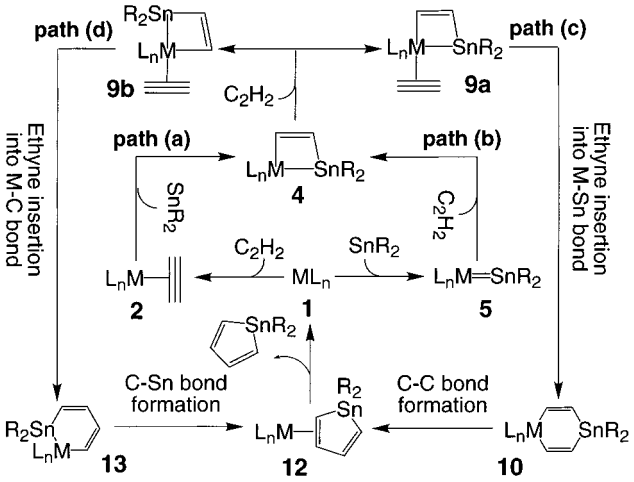

Figure 1. Possible catalytic cycle for stannole formation.

depending upon the position occupied by the incoming ethyne, cis or trans to Sn, after a PH_3 ligand dissociation. In path c, the insertion of ethyne into the M−Sn bond takes place, since **9a** has ethyne cis to Sn. The subsequent step, C−C bond formation, produces the product stannole. In another path d, ethyne in **9b**, being cis to C, is inserted into the M−C bond, which is accompanied by C−Sn bond formation to produce stannole. Pörschke et al. suggested that intermediate **4**, whose stability significantly depends on the metal and the substituent of the phosphine ligand, plays a key role in the catalytic activity.[3b] Only the Pd complex catalyzes the stannole formation; neither the Ni nor the Pt complex does. The catalytic activity increases with the increase in bulkiness of the phosphine ligand. The feature of the reaction profile is thought to depend on the phosphine ligand.

In the present study, we have theoretically investigated the entire catalytic cycle of the stannole formation by means of both density functional theory (DFT) and ONIOM[4] methods, taking account of the effects of metals and ligands on the potential energy surface of the catalytic reaction. Here, we have adopted the $M(PR_3)_2$ (M = Ni, Pd, Pt) complex as a precursor of the catalyst, which is more active than the $(R_2PC_2H_4PR_2)M$ complex, and SnR'_2 as a stannylene. To determine the most favorable path of the entire catalytic cycle for Ni, Pd, and Pt by the DFT method, a model molecule with H for both R and R′ was used. For the investigations of the effects of the substituent of the phosphine ligand on the potential energy surface by the ONIOM method, we used the real molecules with the substituents Me, i-Pr, and t-Bu for R and $CH(SiMe_3)_2$ for R′. Following the explanation of the calculation method, we will discuss the first process of the 1,2-metallastannete intermediate formation and then the ethyne insertion and the reductive elimination of the stannole for Ni, Pd, and Pt. The structural features of the equilibrium structures and the transition states were quite similar among the metals Ni, Pd, and Pt. Therefore, the optimized structures for those metals are discussed together in the same section. In the subsequent section, entire potential energy surfaces consisting of the most favorable paths for Ni, Pd, and Pt are presented. In the last section, the effects of the substituents Me, i-Pr, and t-Bu on P on the potential energy surface for Pd are discussed.

2. Computational Details

All DFT and ONIOM calculations were performed using the Gaussian98 program.[5] The calculations of energetics as well as geometry optimizations for the model molecules were carried out at the B3LYP level of theory, which consists of a hybrid Becke + Hartree−Fock exchange and Lee−Yang−Parr correlation functional with nonlocal corrections,[6] using the basis sets I and II. In the basis set I, we used the lanl2dz basis function implemented by the Gaussian98 program for all atoms. In the basis set II, including polarization functions for C, Sn, and the metals Ni, Pd, and Pt, the 6-31G level for P and H atoms and the 6-31G* level for the C atom were used. For the three metals, we used the triple-ζ construction of the d orbital of the lanl2dz basis functions, augmented by a single set of f polarization functions[7] with the exponents 3.130 (Ni), 1.472 (Pd), and 0.993 (Pt), and the effective core potential (ECP) determined by Hay and Wadt[8] to replace the core electrons except for the 18 electrons in the valence shell. For Sn, the lanl2dz basis functions with a 5d polarization function with the exponent of 0.183[9] and the Hay−Wadt ECP[10] to replace the core electrons except the 4 valence electrons were used.

Upon comparison between the basis sets I and II, we found only small differences in the optimized geometries and energetics for the Ni, Pd, and Pt systems. This indicates that the qualitative results are not dependent on the polarization functions. Therefore, for the model system in the ONIOM calculations, we used the geometries determined at the B3LYP level with the basis set I. For the model molecules calculated at the B3LYP level, only the results with the basis set II are presented. All equilibrium structures and transition states were optimized without any symmetry restrictions, unless otherwise indicated, and identified by the number of imaginary frequencies calculated from the analytical Hessian matrix. The reaction coordinates were followed from the transition state to the reactant and the product by the intrinsic reaction coordinate (IRC) technique.[11] The thermochemical parameters, enthalpy, entropy, and Gibbs free energy, were calculated at the B3LYP/II level with a scale factor of 0.9614[12] for calculated vibrational frequencies at the temperature of 298.15 K.

(4) (a) Dapprich, S.; Komáromi, I.; Byun, K. S.; Morokuma, K.; Frish, M. J. *J. Mol. Struct. (THEOCHEM)* **1999**, *461*−*462*, 1. (b) Humbel, S.; Sieber, S.; Morokuma, K. *J. Chem. Phys.* **1996**, *105*, 1959. (c) Maseras, F.; Morokuma, K. *J. Comput. Chem.* **1995**, *16*, 1170. (d) Matsubara, T.; Sieber, S.; Morokuma, K. *Int. J. Quantum Chem.* **1996**, *60*, 1101. (e) Svensson, M.; Humbel, S.; Froese, R. D. J.; Matsubara, T.; Sieber, S.; Morokuma, K. *J. Chem. Phys.* **1996**, *100*, 19357. (f) Matsubara, T.; Maseras, F.; Koga, N.; Morokuma, K. *J. Chem. Phys.* **1996**, *100*, 2573.

(5) Frisch, M. J.; Trucks, G. W.; Schlegel, H. B.; Scuseria, G. E.; Robb, M. A.; Cheeseman, J. R.; Zakrzewski, V. G.; Montgomery, J. A., Jr.; Stratmann, R. E.; Burant, J. C.; Dapprich, S.; Millam, J. M.; Daniels, A. D.; Kudin, K. N.; Strain, M. C.; Farkas, O.; Tomasi, J.; Barone, V.; Cossi, M.; Cammi, R.; Mennucci, B.; Pomelli, C.; Adamo, C.; Clifford, S.; Ochterski, J.; Petersson, G. A.; Ayala, P. Y.; Cui, Q.; Morokuma, K.; Malick, D. K.; Rabuck, A. D.; Raghavachari, K.; Foresman, J. B.; Cioslowski, J.; Ortiz, J. V.; Stefanov, B. B.; Liu, G.; Liashenko, A.; Piskorz, P.; Komaromi, I.; Gomperts, R.; Martin, R. L.; Fox, D. J.; Keith, T.; Al-Laham, M. A.; Peng, C. Y.; Nanayakkara, A.; Gonzalez, C.; Challacombe, M.; Gill, P. M. W.; Johnson, B.; Chen, W.; Wong, M. W.; Andres, J. L.; Head-Gordon, M.; Replogle, E. S.; Pople, J. A. *Gaussian 98*; Gaussian, Inc.: Pittsburgh, PA, 1998.

(6) (a) Becke, A. D. *Phys. Rev. A* **1988**, *38*, 3098. (b) Lee, C.; Yang, W.; Parr, R. G. *Phys. Rev. B* **1988**, *37*, 785. (c) Becke, D. *J. Chem. Phys.* **1993**, *98*, 5648.

(7) Ehlers, A. W.; Böhme, M.; Dapprich, S.; Gobbi, A.; Höllwarth, A.; Jonas, V.; Köhler, K. F.; Stegman, R.; Velkamp, A.; Frenking, G. *Chem. Phys. Lett.* **1993**, *208*, 111.

(8) Hay, P. J.; Wadt, W. R. *J. Chem. Phys.* **1985**, *82*, 299.

(9) Huzinaga, S. In *Physical SciencesData 16, Gaussian Basis Sets for Molecular Calculations*; Elsevier: Amsterdam, 1984.

(10) Hay, P. J.; Wadt, W. R. *J. Chem. Phys.* **1985**, *82*, 284.

(11) Fukui, K.; Kato, S.; Fujimoto, H. *J. Am. Chem. Soc.* **1975**, *97*, 1.

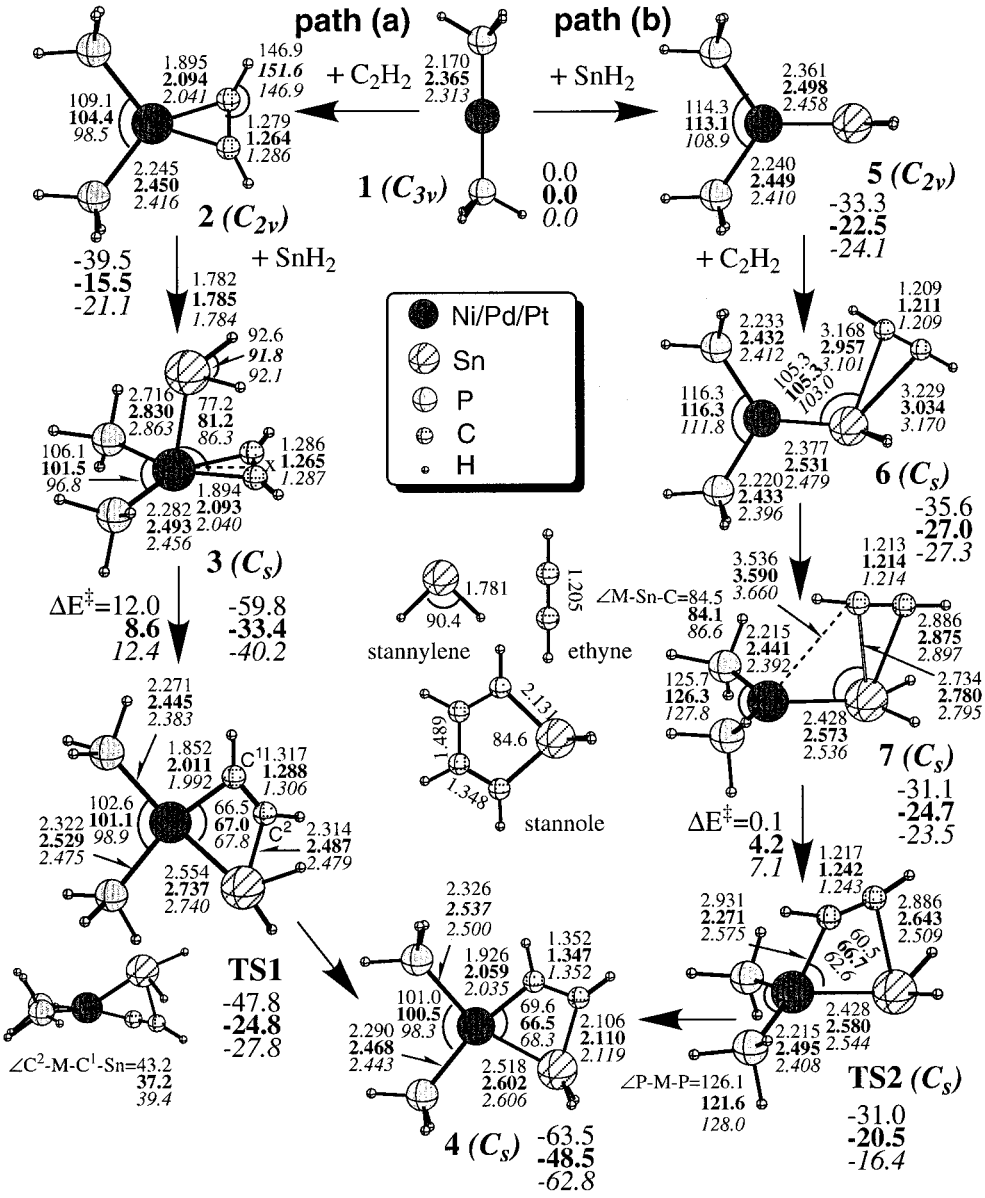

Figure 2. B3LYP/II-optimized structures (in Å and deg) and relative energies (in kcal/mol) of the intermediates and transition states included in paths a and b of the formation of 1,2-metallastannete intermediate **4** from **1**. Numbers in regular, boldface, and italic type are for Ni, Pd, and Pt, respectively. x in **3** represents the midpoint of the two carbon atoms of the coordinated ethyne.

In the ONIOM calculations, the geometries of the real molecule were determined by the combined MO + MM method.[13] The real system was optimized with the universal force field (UFF)[14] fixing the model system except for the substituents Me, i-Pr, and t-Bu for R and CH(SiMe$_3$)$_2$ for R′ attached instead of H. The energies at the geometry calculated by the combined MO + MM method were recalculated at the ONIOM2(B3LYP/lanl2dz:HF/lanl2mb) level.

3. Results and Discussion

3.1. Formation of the 1,2-Metallastannete Intermediate. In the first process of the catalytic cycle, the formation of the 1,2-metallastannete intermediate **4**, we will consider the two possible reaction paths a and b, since the starting complex **1** can react with both ethyne and SnR_2 to afford the ethyne π-complex **2** and stannylene complex **5**, respectively, as mentioned in the Introduction.

Path a. In path a **1** first reacts with ethyne to form the ethyne π-complex **2**. The optimized structures with selected important geometrical parameters and their energies relative to **1** for Ni, Pd, and Pt are presented in Figure 2. The structure of **2** is a square plane with C_{2v} symmetry. Ethyne interacts with the metal through electron σ-donation from the π orbital of ethyne to the mixed orbital of dσ + sp of the metal and electron π-back-donation from the occupied dπ orbital of the metal to the π^* orbital of ethyne, which is well-known as a Dewar−Chatt−Duncanson model.[15] The dπ orbital

(12) Scott, A. P.; Radom, L. *J. Phys. Chem.* **1996**, *100*, 16502.
(13) (a) Kawamura-Kuribayashi, H.; Koga, N.; Morokuma, K. *J. Am. Chem. Soc.* **1992**, *114*, 8687. (b) Maseras, F.; Koga, N.; Morokuma, K. *Organometallics* **1994**, *13*, 4008. (c) Yoshida, T.; Koga, N.; Morokuma, K. *Organometallics* **1996**, *15*, 766. (d) Nozaki, K.; Sato, N.; Tonomura, Y.; Yasutomi, M.; Takaya, H.; Hiyama, T.; Matsubara, T.; Koga, N. *J. Am. Chem. Soc.* **1997**, *119*, 12779.
(14) Rappé, A. K.; Casewit, C. J.; Colwell, K. S.; Goddard, W. A.; Skiff, W. M. *J. Am. Chem. Soc.* **1992**, *114*, 10024.
(15) (a) Dewar, M. J. S. *Bull. Soc. Chim. Fr.* **1951**, C71. (b) Chatt, J.; Duncanson, L. A. *J. Chem. Soc.* **1953**, 2939.

in the P−M−P plane is enhanced by the bend of the P−M−P axis to interact with the π^* orbital of an incoming ethyne,[16] so that ethyne is parallel to the P−M−P axis. The strength of the interaction between the metal and ethyne is reflected in both the C−C bond distance of the coordinated ethyne and the stability of **2**; the C−C bond distance as well as the stability increases with the increase in the interaction in the order Ni > Pt > Pd. The formed π-complex **2** next reacts with the stannylene, SnH_2, leading to the complex **3**. In **3**, SnH_2 occupies the apical position, interacting with the metal by only the donation of the lone-pair electron on Sn to the dσ + sp orbital of the metal. The M−Sn bond distance is, therefore, much longer than that in the stannylene complex **5**, where Sn interacts with the metal by both donation and back-donation (see below). The structure deviates from a true trigonal pyramid, since SnH_2 inclines toward the coordinated ethyne, as shown by the angle ∠Sn−M−X being less than 90°, to have a better overlap in the aforementioned donation interaction between the metal and Sn. The two hydrogens on Sn also incline toward ethyne to have an agostic interaction with the metal, the Sn−H distances being lengthened by 0.01−0.04 Å compared to that in free stannylene. Insertion of SnH_2 into the M−C bond takes place in **3** to form the 1,2-metallastannete intermediate **4**, which has a square-planar structure with C_s symmetry. The twist angle of 7° made by the two planes P−Pd−P and Sn−C−C, which is experimentally observed by the X-ray crystallographic analysis of the analogous 1,2-palladastannete complex $\{(i\text{-}Pr)_2PC_2H_4P(i\text{-}Pr)_2\}Pd(CH{=}CH)Sn\{CH(SiMe_3)_2\}_2$(*Pd−Sn*),[3] could be attributed to the steric repulsion between the bulky substituents, i-Pr on P and $CH(SiMe_3)_2$ on Sn. The insertion of SnH_2 into the M−C bond in the step from **3** to **4** passes through the transition state **TS1**. SnH_2, which is in the apical position, moves toward one of the ethyne carbons, reducing the dihedral angle ∠C^2−M−C^1−Sn to be 40° in **TS1**. The unoccupied p orbital of Sn, to which the electron donation from the M−C bonding orbital initially occurs in this insertion for the M−C bond breaking and the Sn−C bond formation, is already directed to the M−C bonding orbital in **3** to reduce the energy barrier because the SnH_2 moiety is inclined. Thus, the relatively small energy barrier of about 10 kcal/mol[17] for the insertion of SnH_2 into the M−C bond is understandable. It was suggested by the atomic charge analysis that during this insertion the oxidation number of II for both Pd and Sn is unchanged. The difference in natural atomic charge on Pd between **2** and **4** was only 0.09 e. On the other hand, in the step from **1** to **2**, the positive atomic charge increased by 0.40 e, suggesting that Pd(0) is oxidized and becomes Pd(II). In addition to the fact that the M−C bond distance of 1.9−2.0 Å in **2** is quite short, this result indicates that **2** is the metallacycle complex with M(II) rather than the π-complex with M(0).

Path b. In path b **1** first reacts with SnH_2, leading to the stannylene complex **5**, which has a triangular-planar structure with C_{2v} symmetry. The calculated Pd−Sn bond distance of 2.498 Å in the complex **5** is in good agreement with the experimentally observed distance of 2.481 Å by X-ray analysis for the complex $\{(i\text{-}Pr)_2PC_2H_4P(i\text{-}Pr)_2\}Pd{=}Sn\{CH(SiMe_3)_2\}_2$.[3] The interaction between the metal and Sn in **5** would be well expressed by both σ-donation of the lone pair electrons of Sn to the dσ + sp orbital of the metal and π-back-donation from the occupied dπ orbital of the metal to the unoccupied p orbital of Sn:

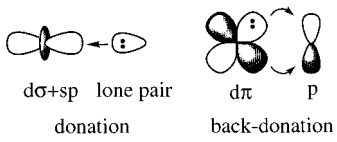

The H−Sn−H axis is perpendicular to the P−M−P axis so that the unoccupied p orbital of Sn interacts with the occupied dπ orbital of metal enhanced by the bend of the P−M−P axis. The interaction between the metal and Sn by both donation and back-donation in **5** might be similar to that in the Fisher type carbene complex.[18] Because the electrons contributing to the π-back-donation are thought to be relatively localized on the dπ orbital of the metal rather than on the p orbital of Sn, due to the fact that the small rotation energy around the Pd−Sn axis on **5** is calculated to be 6.0 kcal/mol, which indicates that the interaction by the π-back-donation is weak. In the analogous carbene complex, a much larger rotation energy of 16.7 kcal/mol was calculated, indicating that the π-back-donation is strong. The positive natural atomic charge on Pd was larger by 1.82 e in the carbene complex than in the stannylene complex, supporting this assumption, which would be ascribed to the fact that the electronegativity is much larger for C (2.55)[19] than for Sn (1.96).[19] The stannylene complex **5** as well as the ethyne π-complex **2** showed the sequence of the stability Ni > Pt > Pd.

In **5**, the coordination of ethyne takes place not on the metal but on Sn to form **6**. The coordinated ethyne largely inclines toward hydrogens of stannylene due to the steric repulsion with the PH_3 ligand. We did not find any structure with ethyne coordinated to the metal or to the bridge site of the M−Sn bond, although the possibility of μ-alkyne complexes has been suggested both experimentally[3b] and theoretically.[20] The interaction caused only by the donation of the electrons in the π orbital of ethyne to the unoccupied p orbital of Sn is very weak, as shown by the very long Sn−C bond distances and the only slightly elongated ethyne C−C bond distance, because this donation is disturbed by donation from the dπ orbital of metal to the p orbital of Sn. In other words, the σ-donation from ethyne to Sn weakens the π-back-donation from the metal to Sn. As expected, the coordination of ethyne to Sn lowered the energy required for the rotation around the M−Sn bond. For example, for Pd, the energy required for the rotation

(16) (a) Low, J. J.; Goddard, W. A., III. *J. Am. Chem. Soc.* **1984**, *106*, 6928. (b) Obara, S.; Kitaura, K.; Morokuma, K. *J. Am. Chem. Soc.* **1984**, *106*, 7482. (c) Saillard, J.-Y.; Hoffmann, R. *J. Am. Chem. Soc.* **1984**, *106*, 200.

(17) In the other insertion, for example, CO insertion into the M−R (M = Pd, Pt; R = H, Me) bond, energy barriers much higher than 10 kcal/mol have been reported. See: (a) Sakaiki, S.; Kitaura, K.; Morokuma, K. *J. Am. Chem. Soc.* **1983**, *105*, 2280. (b) Koga, N.; Morokuma, K. *J. Am. Chem. Soc.* **1985**, *107*, 7230. (c) Koga, N.; Morokuma, K. *J. Am. Chem. Soc.* **1986**, *108*, 6536.

(18) Fischer, E. O.; Maasbol, A. *Angew. Chem., Int. Ed. Engl.* **1964**, *3*, 580.

(19) *The Elements*, 2nd ed.; Emsley, J., Ed.; Oxford University Press: New York, 1991.

(20) Hoffman, D. M.; Hoffman, R.; Fisel, C. R. *J. Am. Chem. Soc.* **1982**, *104*, 3858.

around the M−Sn bond was 6.0 kcal/mol in **5**, as mentioned above, but it is reduced to be only 2.3 kcal/mol in **6**. Therefore, in the step from **6** to **7**, rotation of the $M(PH_3)_2$ group by 90° around the M−Sn bond takes place to weaken the π-back-donation from the dπ orbital of metal to the p orbital of Sn and strengthen the donation from the π orbital of ethyne to the p orbital of Sn. Thus, in **7**, the M−Sn bond distance becomes longer, whereas the Sn−C distances become shorter and ethyne inclines back to come closer to the metal. Although we did not locate the TS between **6** and **7**, it was found by following the reaction coordinate that both the structure and energy of the TS were extremely close to those of **7**. In **7**, the triple bond of ethyne is already initially activated by the interaction with Sn by the electron donation from the ethyne π orbital to the Sn p orbital, as presented in the orbital illustration

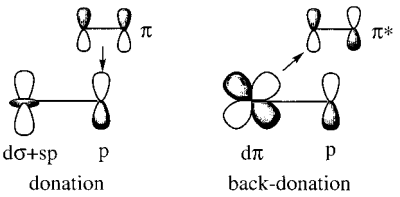

In addition, the electron back-donation from the metal dπ orbital to the ethyne π* orbital breaks the ethyne triple bond to form the M−C bond through the transition state **TS2**. By these consecutive stepwise interactions of ethyne with the sites on bimetallic M−Sn, where the electron movement between M and Sn would be easy, the energy barrier of the ethyne addition to the M−Sn double bond is efficiently lowered. The ethyne coordination to Sn makes the rotation of the $M(PH_3)_2$ group easy, and the energy barrier of ethyne addition to the M−Sn double bond is reduced by this rotation. The energy barrier for the ethyne addition from **7** to **4** was calculated to be less than 10 kcal/mol for all three metals and was only 0.1 kcal/mol, as for Ni. Thus, path b is much more favorable than path a for Ni, Pd, and Pt.

After passing through **TS2**, the $M(PH_3)_2$ group rotates back to produce **4**. The M−Sn single bond in **4** is longer by 0.10−0.15 Å than the M−Sn double bond in **5**. Although one would recognize a slight sp^3 hybridization on Sn with the attached hydrogens moved away from the ethyne carbon in **4**, it seems not to be completed because of the large deviation of Sn from a regular tetrahedral structure keeping in part the character of the lone pair electron. The structures at the stationary point from **5** to **4** seem to be the serial snapshots in the addition reaction of ethyne to the M−Sn double bond. Without rotation of $M(PH_3)_2$ group around the M−Sn bond in **6**, no TS was located in this ethyne addition.

3.2. Ethyne Insertion into the M−Sn bond vs Insertion into the M−C Bond. Since the dissociation of phosphine ligand cis or trans to Sn in **4** leads to the coordinatively unsaturated intermediate **8a** or **8b**, we have two possible reaction paths, c and d. The empty site formed by the phosphine dissociation is kept at the same position and is provided for the coordination of the incoming ethyne, although the angles ∠P−M−C in **8a** and ∠P−M−Sn in **8b** become slightly larger to relax the steric contact of PH_3 with the metallacycle ring, as displayed in Figures 3 and 4.

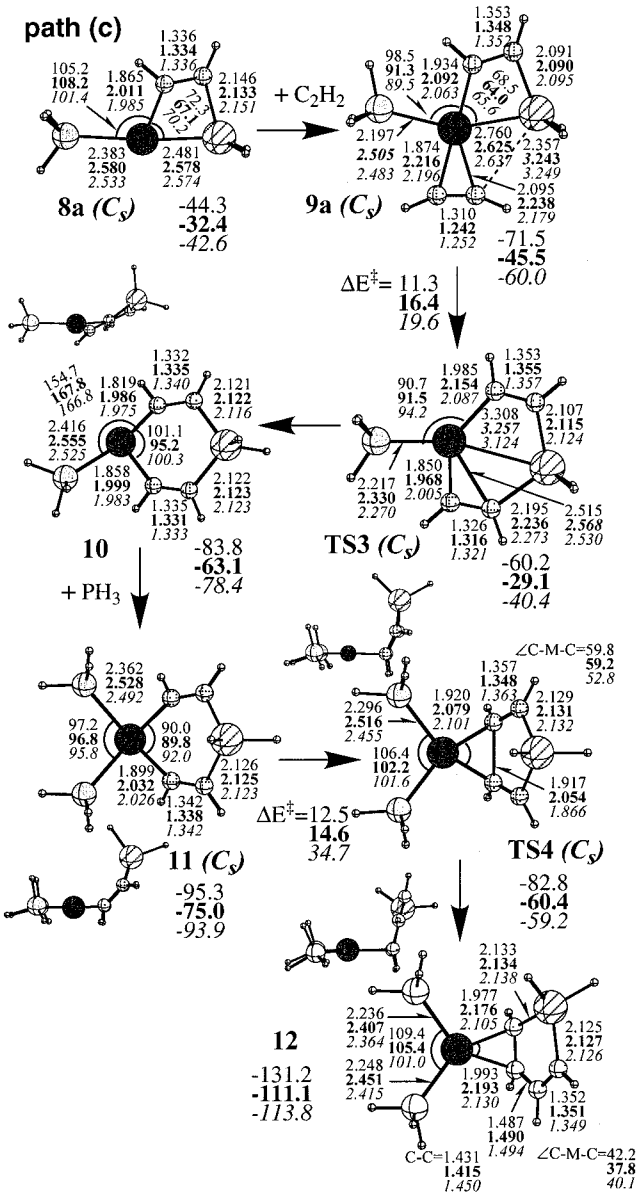

Figure 3. B3LYP/II-optimized structures (in Å and deg) and relative energies (in kcal/mol) of the intermediates and transitions states included in path c, consisting of PH_3 dissociation (**4** → **8a**), ethyne coordination (**8a** → **9a**), ethyne insertion into the M−Sn bond (**9a** → **10**), PH_3 recoordination (**10** → **11**), and C−C bond formation (**11** → **12**).

8a is less stable by about 6 kcal/mol than **8b** due to a trans and/or cis influence of C and Sn to the PH_3 ligand, but this tendency is reversed in **9**. The coordinated ethyne is parallel to the four-membered metallacycle ring in **9a** but perpendicular in **9b** to avoid the large steric contact with the close CH moiety of the metallacycle ring. As a result, the M−ethyne interaction is weaker in **9b** than in **9a**, as shown by the distance being much longer in **9b** than in **9a**. Indeed, the stabilization by ethyne coordination is smaller by 6−15 kcal/mol in **9b** than in **9a**.

Path c. In **9a**, where ethyne is cis to Sn, the insertion of ethyne into the M−Sn bond takes place. One important factor in determining the reactivity of the ethyne insertion would be the orientation of the coordinated ethyne. Although a perpendicular orientation to the

metallacycle ring was somewhat preferred for geometrical reasons for Ni due to the strong steric repulsion between the coordinated ethyne and the metallacycle ring, a parallel orientation was found for all three metals. Ethyne insertion into the M−Sn bond occurs, keeping the C_s symmetry, which is similar to the previous theoretical reports for alkyne[21] and olefin[22] insertion into the metal−SnR_3 or into the metal−SiR_3 bond. Since the ethyne insertion, which is accompanied by the breaking of the M−Sn and ethyne triple bonds and the formation of the M−C and Sn−C bonds, takes place by the electron donation from the ethyne π orbital to the M−Sn antibonding orbital and electron back-donation from the M−Sn bonding orbital to the ethyne π^* orbital, as presented below, the transition state, **TS3**, should have a planar structure with C_s symmetry:

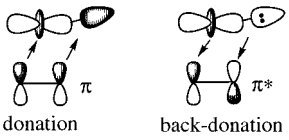

However, it should be noted that the energy barrier of less than 20 kcal/mol (16.4 kcal/mol for Pd) is small compared with that of more than 20 kcal/mol for the ethyne insertion into the Pd−SnH_3 bond previously reported by Hada et al.[21] This would be ascribed to the character of the M−Sn bond being different from the covalent bond of metal−SnR_3 in the previous system. The rigid four-membered metallacycle ring does not allow the completion of sp^3 hybridization on Sn also in **9a**, as mentioned above. Accordingly, the donating character of the lone pair electron of Sn to the $d\sigma + sp$ orbital of the metal would still remain. In **TS3**, both M−C and M−Sn bond distances are largely elongated by 0.3−0.4 Å and by 0.5−0.6 Å, respectively, compared to those in **9a**, and the Sn−C bond is almost formed, as shown by the distance being slightly longer than that in **10**. In **10**, the sp^3 hybridization on Sn is completed. The metal in the six-membered ring is out of its plane, because not only the sp^2 orbital but also the π orbital of carbon contributes to the bonding with the metal to obtain more stabilization by geometrical means.

Path d. On the other hand, in **9b**, where ethyne is cis to C, the insertion of ethyne into the M−C bond takes place. Since the orientation of the coordinated ethyne is perpendicular to the four-membered metallacycle ring, ethyne has to change its orientation for the insertion by rotation around the axis connecting the metal and the midpoint of two carbons of ethyne. This rotation energy of ethyne, however, was only 1.2 kcal/mol for Pd, indicating that the large energy barrier for the insertion mentioned below does not arise from the ethyne rotation. The structure of the transition state, **TS5**, largely deviates from planarity in contrast to that of **TS3**, because the π orbitals of carbon of both ethyne and the metallacycle ring participate to stabilize the TS. Nevertheless, the energy barrier of ethyne insertion into the M−C bond is larger than that of ethyne insertion into the M−Sn bond, and the difference is about 10 kcal/mol, except for 1.1 kcal/mol for Ni. This result is in agreement with the previous experimental findings that ethyne insertion into the M−C bond rarely occurs;[23] in contrast, ethyne insertion into the M−Si or M−Sn bond easily takes place.[24] We have also reported the large energy barrier of 40 kcal/mol for ethylene insertion into the M−C bond in the Ru complex system.[25] In **TS5**, the C−C bond distance is still much longer compared to that of **13**. Because of the changing of the orientation of ethyne, both M−ethyne-C and M−metallacycle-C bond distances become shorter compared to those in **9b**, except for the M−metallacycle-C bond distance for Ni.

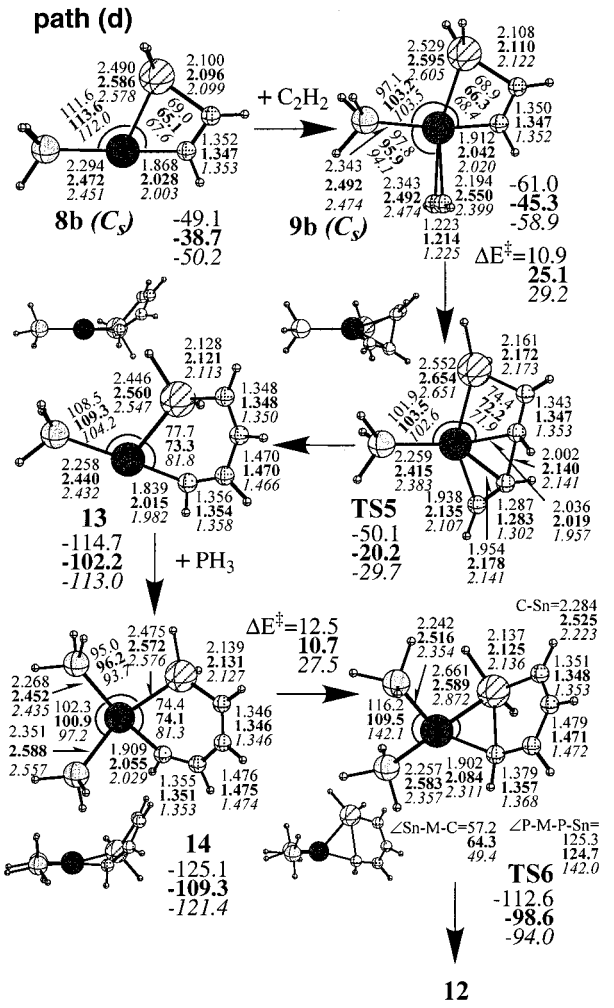

Figure 4. B3LYP/II-optimized structures (in Å and deg) and relative energies (in kcal/mol) of the intermediates and transition states included in path d, consisting of PH_3 dissociation (**4** → **8b**), ethyne coordination (**8b** → **9b**), ethyne insertion into the M−C bond (**9b** → **13**), PH_3 recoordination (**13** → **14**), and Sn−C bond formation (**14** → **12**).

3.3. C−C vs C−Sn Bond Formation To Produce Stannole. The dissociated phosphine in the prior step,

(21) Hada, M.; Tanaka, Y.; Ito, M.; Murakami, M.; Amii, H.; Ito, Y.; Nakatsuji, H. *J. Am. Chem. Soc.* **1994**, *116*, 8754.

(22) (a) Sakaki, S.; Ogawa, M.; Musashi, Y.; Arai, T. *J. Am. Chem. Soc.* **1994**, *116*, 7258. (b) Sakaki, S.; Mizoe, N.; Sugimoto, M. *Organometallics* **1998**, *17*, 2510.

(23) (a) Tohda, Y.; Sonogashira, K.; Hagihara, N. *J. Chem. Soc., Chem. Commun.* **1975**, 54. (b) Mann, B. E.; Bailey, P. M.; Maitlis, P. M. *J. Am. Chem. Soc.* **1975**, *97*, 1275. (c) Kelly, E. A.; Bailey, P. M.; Maitlis, P. M. *J. Chem. Soc., Chem. Commun.* **1977**, 289. (d) Clark, H. C.; Milne, C. R. C.; Wong, C. S. *J. Organomet. Chem.* **1977**, *136*, 265.

(24) (a) Pereyre, M.; Quintard, J.-P.; Rahm, A. In *Tin in Inorganic Synthesis*; Butterworth: London, 1987; pp 21−23. (b) Harrison, P. G. In *Chemistry of Tin*; Blackie: Glasgow, U.K., 1989; pp 159−160. (c) Yamashita, H.; Tanaka, M.; Goto, M. *Organometallics* **1993**, *12*, 988.

(25) Matsubara, T.; Koga, N.; Musaev, D. G.; Morokuma, K. *Organometallics* **2000**, *19*, 2318.

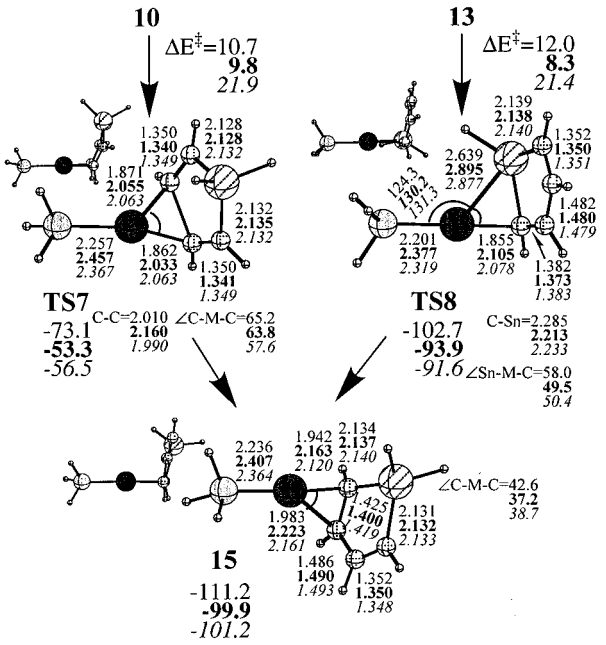

Figure 5. B3LYP/II-optimized structures (in Å and deg) and relative energies (in kcal/mol) of the intermediate and transition states in C−C and Sn−C bond formation without recoordination of the PH_3 ligand.

ethyne insertion, will recoordinate to stabilize the intermediate **10** or **13**, forming **11** or **14**, before C−C or C−Sn bond formation. However, as we have reported for C−H or C−C bond formation in the Ru complex system,[25] C−C or C−Sn bond formation without recoordination of the phosphine ligand would require a smaller energy barrier compared to that with the recoordination of the phosphine ligand. Therefore, we examined the C−C(path c) and C−Sn(path d) bond formations with and without recoordination of a phosphine ligand.

Path c. The metal in the six-membered ring in **11**, compared to that in **10**, moves out more from its plane since the contribution of the π orbital of carbon in the interaction with the metal increases to get the stabilization because the ∠C−M−C angle becomes smaller by the recoordination of the phosphine ligand. This feature becomes significant in the transition state of the C−C bond formation, **TS4**, where the plane of stannole is almost perpendicular to the P−M−P plane. In the product **12**, the C−C π bond of stannole coordinates to the metal.

The optimized structures and their relative energies in the C−C bond formation without PH_3 recoordination is presented in Figure 5. In comparison with the corresponding structures with the recoordinated PH_3 ligand, some differences will be found. The geometrical symmetry disappeared in the transition state, **TS7**, and the C−C and M−C bond distances are affected by the loss of one PH_3 ligand. A significant difference appears in the C−C bond distance, which is 0.1 Å longer than that in **TS4**, indicating that **TS7** is a more early transition state. The ∠C−M−C angle is also 5° larger in **TS7** than in **TS4**. The C−C bond distance in **15** is 0.01−0.03 Å shorter than that in **12**, because the interaction between the metal and the double bond of stannole dominantly through the electron back-donation from the dπ orbital of the metal to the π* orbital of the C−C double bond in the d^{10} metal complex is reduced by the loss of one of electron donative PH_3 ligands. However, the coordination features of stannole in both the transition state **TS7** and stannole-coordinated complex **15** are similar to those in the corresponding complexes with two PH_3 ligands.

The energy barrier for C−C bond formation is smaller with one PH_3 ligand than with two PH_3 ligands, although the potential energy surface is less stable in energy with one PH_3 ligand than with two PH_3 ligands. The difference in energy barrier between those reactions with one and two PH_3 ligands increases in the order Pt (12.8 kcal/mol) > Pd (4.8 kcal/mol) > Ni (1.8 kcal/mol).

Path d. In **14**, C−Sn bond formation takes place. In the transition state **TS6**, the P−M−P and Sn-M−C planes surprisingly twist with respect to each other to have a dihedral angle of 124−142°. In contrast to this, in **TS4**, the transition state in the C−C bond formation, the C−M−C plane is almost in the same plane as the P−M−P plane, which is similar to the computational results reported so far for H−H, H−C, and C−C bond formation in the Pt and Pd complexes.[16,26] This unique feature is quite similar to that of **3**, where the C−C ethyne bond coordinates to the metal instead of carbon and is considered to originate from the interaction of Sn at the apical position with the metal mainly by the donation of the lone pair electron to the metal, because the orbital character of the lone pair electron would still remain on Sn as mentioned above. This change in geometrical configuration from **14** to **TS6** would efficiently weaken the M−Sn bond, as seen in the long distance of the M−Sn bond in **3**, and reduce the energy barrier by the stabilization obtained by such donation interaction. In fact, the energy barrier is smaller by 4−7 kcal/mol in the Sn−C bond formation than in the C−C bond formation for Pd and Pt, whereas the energy barriers are comparable for Ni.

The structural feature of **TS8**, with one PH_3 ligand, was similar to that of **TS6**, with two PH_3 ligands, as presented in Figure 5. The energy barrier with one PH_3 ligand was smaller than that with two PH_3 ligands, although its potential energy surface is less stable in energy, which is similar to the case of the C−C bond formation.

3.4. Entire Potential Energy Surface of the Catalytic Stannole Formation. The entire potential energy surfaces for the catalytic stannole formation by Ni, Pd, and Pt complexes, which consist of the most favorable paths, are presented in Figure 6. For all three metals, Ni, Pd, and Pt, the potential energy surface is constructed by paths b and c, avoiding the largest energy barrier in the ethyne insertion into the M−C bond for Pd and Pt and in the C−Sn bond formation for Ni. Here, the C−C bond formation takes place without the recoordination of the dissociated PH_3 ligand in the prior step, ethyne insertion into the M−Sn bond. Hence, the stannole-coordinated complex **12** is formed from **15** by the PH_3 recoordination. The addition of SnR'_2 to **1** first leads to the stannylene complex **5** and the subsequent ethyne addition to the M−Sn double bond of **5**

(26) (a) Low, J. J.; Goddard, W. A., III. *J. Am. Chem. Soc.* **1984**, *106*, 6928. (b) Low, J. J.; Goddard, W. A., III. *J. Am. Chem. Soc.* **1984**, *106*, 8321. (c) Low, J. J.; Goddard, W. A., III. *Organometallics* **1986**, *5*, 609. (d) Low, J. J.; Goddard, W. A, III. *J. Am. Chem. Soc.* **1986**, *108*, 6115.

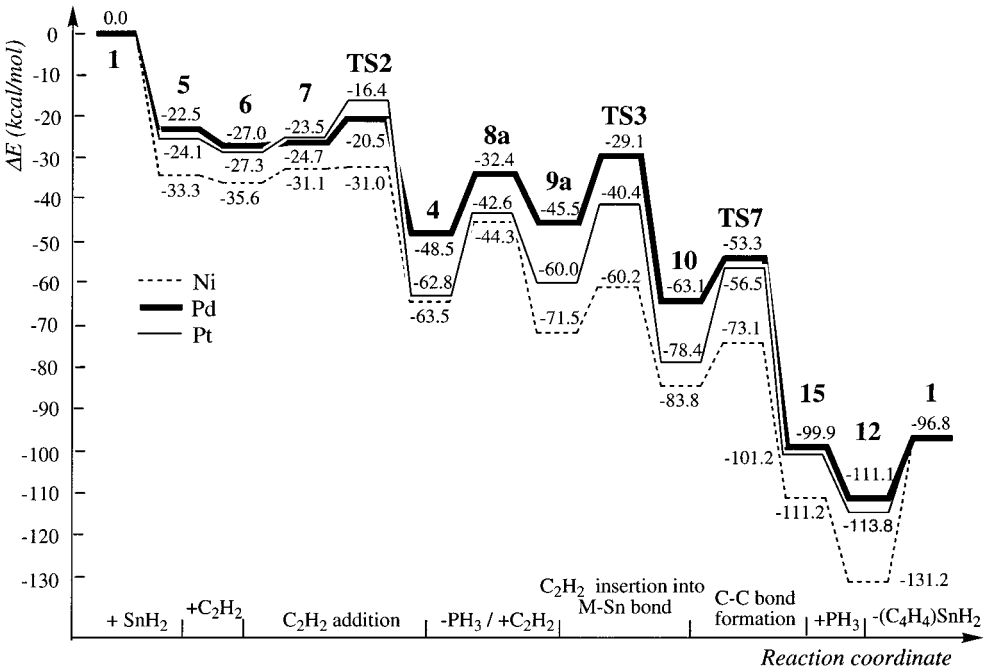

Figure 6. B3LYP/II potential energy surfaces of the catalytic cycle of stannole formation consisting of the most favorable paths b and c for Ni, Pd, and Pt. The dotted, boldface, and normal lines are for Ni, Pd, and Pt, respectively.

leads to the 1,2-metallastannete intermediate **4**. In this consecutive reaction from **1** to **4**, an energy of only less than 10 kcal/mol is needed to overcome the energy barriers. The potential energy surface of the formation of 1,2-metallastannete intermediate **4** is quite smooth compared to that of the subsequent reaction process, ethyne insertion into the M−Sn bond and C−C bond formation. For Ni and Pd, ethyne insertion requires the largest energy barriers of 11.3 and 16.4 kcal/mol, respectively. On the other hand, for Pt, the C−C bond formation requires the largest energy barrier of 21.9 kcal/mol. For all three metals, the transition state, **TS2**, in the ethyne addition to the M−Sn double bond was located at the highest point on the entire potential energy surface. On the basis of the potential energy surfaces for Ni, Pd, and Pt, one can predict that the reactivity follows the sequence Ni > Pd > Pt, since the entire potential energy surface is stable in energy with the order Ni > Pd > Pt, and the energy barriers on the entire potential energy surface have the opposite order. According to the experimental observation by Pörschke et al., Pd catalyzes the stannole formation and neither Ni nor Pt does, because the intermediate **4**, which can be independently experimentally synthesized, is too stable for Pt to react with an additional ethyne, which is too unstable and breaks, exhibiting an undesired reactivity for Ni. Therefore, only with Pd catalysis is the stannole formation attained.[3b] The discrepancy in the stability order in **4** between the experimental and calculated results might originate from the peculiar property of **4** which appears in the solution. In practice, the calculations were performed for the gas phase.

The pre-dissociation of one phosphine ligand in **4** to form **8** for the ethyne insertion and the dissociation of stannole in **12** to reproduce the starting complex **1** require a relatively large energy of 10−20 kcal/mol. If we take the entropy effect into consideration in such dissociation steps where the coordination number decreases, the energy needed for the dissociation would be reduced, as we showed in a previous paper for the Rh complex system.[27] In fact, the Gibbs free energy calculated at the B3LYP/II level for Pd showed the small energy barriers of 1.8 and 4.5 kcal/mol for the steps from **4** to **8a** and from **12** to **1**, respectively, as presented in Table 1.

Table 1. Calculated Potential Energies (Δ*E*), Enthalpies (Δ*H*), Entropies (TΔ*S*), and Gibbs Free Energies (Δ*G*) Relative to 1 in kcal/mol for the Equilibrium Structures and Transition States for Pd Included in Paths b and c

structure	Δ*E*	Δ*H*[a]	*T*Δ*S*[a]	Δ*G*[a]
1	0.0	0.0	0.0	0.0
5	−22.5	−20.6	−6.4	−14.2
6	−27.0	−24.1	−14.5	−9.6
7	−24.7	−22.5	−16.4	−6.1
TS2	−20.5	−19.0	−16.2	−2.8
4	−48.5	−45.1	−21.2	−23.9
8a	−32.4	−30.2	−8.1	−22.1
9a	−45.5	−42.2	−18.5	−23.7
TS3	−29.1	−26.2	−21.7	−4.5
10	−63.1	−59.1	−20.4	−38.7
11	−75.0	−69.0	−31.7	−37.3
TS4	−60.4	−55.7	−31.1	−24.6
12	−111.1	−103.9	−30.5	−73.4
1	−96.8	−90.9	−22.0	−68.9
TS7	−53.3	−49.8	−20.8	−29.0
15	−99.9	−94.0	−20.8	−73.2

[a] Δ*H*, *T*Δ*S*, and Δ*G* = Δ*H* − *T*Δ*S* were calculated at 298.15 K.

The entire energy surface is shifted up and the feature of the energy surface is changed in the ethyne coordination (**5** → **6**) and the C−C bond formation by the entropy effect. The exothermic reaction from **5** to **6** becomes endothermic. In the C−C bond formation, the energy surface without the recoordination of the PH_3 ligand becomes lower than that with the recoordination of PH_3 ligand. This also suggests that the C−C bond formation is more favorable with one phosphine ligand than with two phosphine ligands.

(27) Matsubara, T.; Koga, N.; Ding, Y.; Musaev, D. G.; Morokuma, K. *Organometallics* **1997**, *16*, 1065.

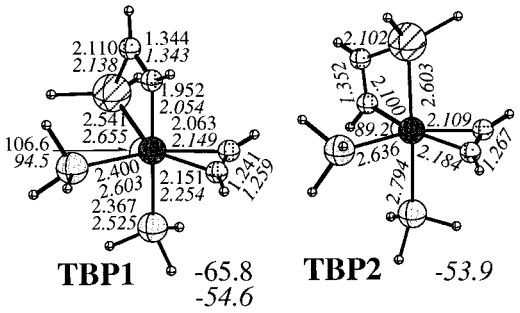

Figure 7. B3LYP/II-optimized structures of the five-coordinated TBP structures **TBP1** and **TBP2** for Ni and Pt formed by ethyne coordination to **4**.

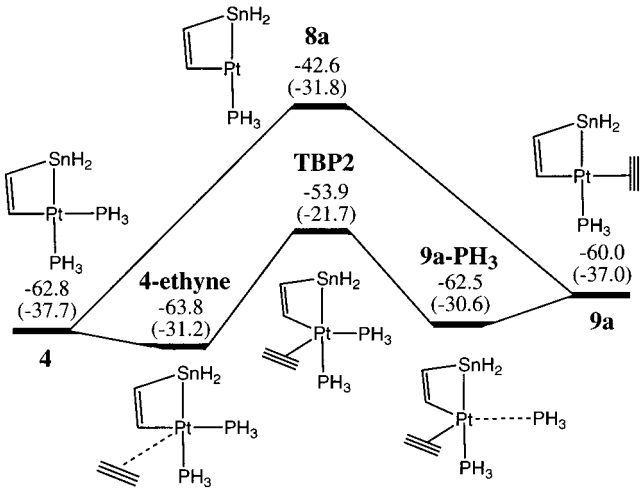

Figure 8. B3LYP/II potential energy surfaces (in kcal/mol) for a PH_3 ligand replacement by ethyne in **4** by the two possible dissociative (**4** → **8a** → **9a**) and associative (**4** → **4-ethyne** → **TBP2** → **9a-PH$_3$** → **9a**) mechanisms. The numbers in parentheses are Gibbs free energies (in kcal/mol) calculated at 298.15 K.

Although we were restricted to only the three- and four-coordinated complexes in the present work, another possible replacement of PH_3 by ethyne by an associative mechanism through a five-coordinated trigonal bipyramidal (TBP) structure can be considered in the step from **4** to **9a**. It is known that the TBP structure is nonrigid and the rearrangement of the coordination configuration is easy.[28] Since the ethyne coordinates parallel to the Sn−M−P or C−M−P axis, two isomers of TBP structure exist. For Pd, no TBP structure existed as an equilibrium structure because of the dissociation of the PH_3 ligand, even if the basis set including a polarization function, 6-31G*, was used for P. However, **TBP1** for Ni and both **TBP1** and **TBP2** for Pt were found, as presented in Figure 7.

For Pt, **TBP1**, where ethyne is parallel to the Sn−Pt−P axis, was slightly more stable in energy than **TBP2**, where ethyne is parallel to the C−Pt−P axis. The potential energy surface of the associative replacement of the PH_3 ligand by ethyne in **4** passing through **TBP2** to form **9a** was examined for Pt and is presented in Figure 8 together with that of the dissociative path.

There exist equilibrium structures, **4-ethyne** between **4** and **TBP2**, where ethyne is weakly bound to Pt, and **9a-PH$_3$** between **TBP2** and **9a**, where PH_3 is weakly bound to Pt. In both paths from **TBP2** to **4-ethyne** and from **TBP2** to **9a-PH$_3$**, a quite small energy barrier of less than 1 kcal/mol was found, by following the reaction coordinate with the variables of the distances of Pt−ethyne and Pt−PH_3. Therefore, the energy barrier in the step from **4-ethyne** to **TBP2** was estimated to be about 10 kcal/mol. Although **TBP2** is more stable in energy than **8a** by 11.3 kcal/mol, the entropy effect makes the five-coordinated complexes **TBP2**, **4-ethyne**, and **9a-PH$_3$** unstable while making the three-coordinated complex **8a** stable. The Gibbs free energy showed that **TBP2**, **4-ethyne**, and **9a-PH$_3$** are less stable than **8a**, suggesting that the dissociative replacement of the PH_3 ligand by ethyne is more favorable than the associative one. We did not find any TS in the ethyne insertion into the Pt−Sn bond in **TBP2**, which is connected to the intermediate **11**, because of a PH_3 ligand dissociation. This suggests that the ethyne insertion proceeds through the four-coordinated transition state **TS3** from **9a**.

3.5. Effects of the Substituent of the Phosphine Ligand on the Potential Energy Surface of the Catalytic Cycle. It is usually expected that the potential energy surface of the catalytic cycle would be affected by the substituent of the ligand. In the present case, as predicted by Pörschke et al.,[3b] it is intuitively considered that the feature of the potential energy surface of the part of the catalytic cycle, especially after the formation of 1,2-metallastannete intermediate **4**, would depend on the steric effect of the substituent on P and Sn. The steric effect of the substituent on P and Sn seems not to affect so much the potential energy surface of path b, judging from the geometric configuration of the transition state as well as the equilibrium structures involved in path b. In ethyne addition to the M−Sn double bond, the Sn−C−C plane is perpendicular to the P−M−P plane, which successfully avoids the steric repulsion between ethyne and the bulky substituents on P. Therefore, we performed the ONIOM2 energy calculations for the structures of path c for Pd obtained by the combined MO + MM method using R = Me, i-Pr, t-Bu and R′ = $CH(SiMe_3)_2$ to find out qualitatively how the potential energy surface of path c is changed by the ligand effects. The ONIOM2(B3LYP:HF) potential energy surfaces in the case of R = Me, i-Pr, t-Bu with R′ = $CH(SiMe_3)_2$ are presented together in Figure 9 in comparison with that in the case of R, R′ = H.

When H for R and R′ is replaced by Me and $CH(SiMe_3)_2$, respectively, the entire potential energy surface becomes slightly more stable in energy by the electronic effect of Me and $CH(SiMe_3)_2$. The energy barrier in the ethyne insertion also becomes smaller because the steric repulsion between the substituents, Me on P, and ethyne and the metallacycle ring is larger in **9a′** than in **TS3′**. Also in the case of R = Me, the potential energy surface of the C−C bond formation is more stable in energy with two phosphine ligands than with one phosphine ligand, although the energy barrier is larger with two phosphine ligands than with one phosphine ligand. When R is i-Pr, the feature of the potential energy surface is different from that in the case of R = Me due to both the electronic and steric effects of i-Pr being larger than those of Me. The entire potential energy surface is more stable in energy than

(28) Koga, N.; Jin, S. Q.; Morokuma, K. *J. Am. Chem. Soc.* **1988**, *110*, 3417.

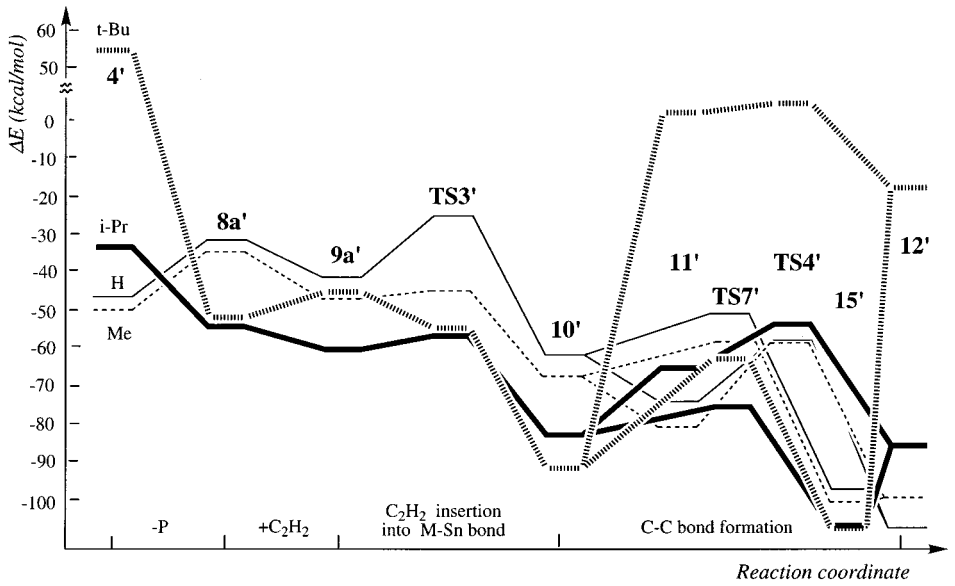

Figure 9. ONIOM2(B3LYP:HF) potential energy surfaces of path c for Pd. The model ($Pd(PH_3)_2$ and SnH_2) and real ($Pd(PR_3)_2$ (R = Me, i-Pr, t-Bu) and SnR'_2 (R′ = $CH(SiMe_3)_2$) molecules were used. The C−C bond formation reactions both with and without recoordination of a PH_3 ligand are presented.

that for Me. The dissociation of the phosphine ligand in **4′** to produce **8a′** is exothermic, because the stabilization energy gained by the reduction of the steric stress is larger than the loss of the bonding energy by the phosphine ligand dissociation. The ethyne insertion requires a small energy barrier for the same reason as the case of Me. In contrast to the case of H or Me, the potential energy surface of the C−C bond formation is more stable in energy with one phosphine ligand than with two phosphine ligands because the recoordination of $P(i\text{-}Pr)_3$ causes a large destabilization due to the large steric effect of $P(i\text{-}Pr)_3$, which enhances the reaction with one phosphine ligand with the smaller energy barrier. Therefore, the potential energy surface of **4′** → **8a′** → **9a′** → **TS3′** → **10′** → **TS7′** → **15′** → **12′** is quite smooth. The energy barrier of 8.8 kcal/mol in the C−C bond formation is larger than that of 2.1 kcal/mol in the ethyne insertion, suggesting the shift of the step which has the highest energy barrier from the ethyne insertion to the C−C bond formation. In the case of R = t-Bu, the four-coordinated intermediates and the transition state, **4′**, **9a′**, **11′**, **12′**, and **TS4′**, are very unstable in energy compared with those in the case of R = i-Pr because the steric effect of t-Bu is too large. Accordingly, the C−C bond formation with one phosphine ligand is obviously energetically more favorable than that with two phosphine ligands. The energy barrier in the C−C bond formation is larger compared with the case for i-Pr, because the larger steric repulsion between substituents R and R′ is more sensitively reflected in **TS7′** than in **10′** due to the geometrical difference between **TS7′** and **10′**, as mentioned above. The distance between the substituents, R and R′, is much shorter in **TS7′** than in **10′**. Consequently, the highest catalytic activity of the substituent i-Pr was suggested by its energetically stable potential energy surface in addition to the fact that the energy barrier required is the smallest. The sequence of the reactivity was predicted to be i-Pr > Me > t-Bu, although there is no experimental result for t-Bu. Of course, it should be noted that the steric effect tends to be overestimated with an increase in the bulkiness of R when we adopt the combined MO + MM method for the optimizations. However, we believe that this analysis for the potential energy surface of the catalytic reaction considering the electronic and steric effects of the ligand supports the catalyst design.

Concluding Remarks

The reaction mechanism of the stannole formation from two ethynes and one stannylene of SnR'_2 catalyzed by the phosphine-coordinated complexes $M(PR_3)_2$ (M = Ni, Pd, Pt) was theoretically studied by means of the DFT method (B3LYP) using a model molecule with R, R′ = H. The reaction proceeds via 1,2-metallastannete intermediate **4**. In the formation of **4**, the stannylene complex **5** is formed first and then ethyne addition to the M−Sn double bond in **5** takes place to form **4** with a small energy barrier. Subsequent ethyne insertion into the M−Sn bond and C−C bond formation to produce stannole requires a larger energy barrier. The highest point in the entire potential energy surface was found at the transition state **TS2** in the ethyne addition to the M−Sn double bond. On the basis of the potential energy surface, the sequence of the catalytic activity was predicted to be Ni > Pd > Pt. The effects of the substituents R on P, Me, i-Pr, and t-Bu, on the potential energy surface were also examined using the real molecule, where $CH(SiMe_3)_2$ was used for R′ of stannylene, by the ONIOM method. As a result, it was predicted that the substituent i-Pr is the best as the catalyst for the present reaction.

Acknowledgment. Part of the calculations were carried out at the Computer Center of the Institute for Molecular Science of Japan. R.S. acknowledges a Postdoctoral Fellowship from the Institute for Fundamental Chemistry.

Supporting Information Available: Listings giving the optimized Cartesian coordinates of all equilibrium structures and transition states presented in this paper. This material is available free of charge via the Internet at http://pubs.acs.org.

OM000487K